A True 1D Analysis of a Klystron Amplifier

Robson K. B. e Silva
Nuclear and Energy Research Institute – IPEN
Av. Prof. Lineu Prestes, 2242 – São Paulo, SP, Brazil
rkeller@usp.br

Cláudio C. Motta
University of Sao Paulo
Av. Prof. Lineu Prestes, 2468 – São Paulo, SP, Brazil
ccmotta@usp.br

Abstract—**This paper presents a large-signal analysis of a klystron amplifier. It is used lagrangian approach and disk model theory in a one-dimensional analysis with emphasis in the effects of the presence of the space-charge force. After showing the result in the free space without considering the space-charge force, is added one that consider this force based on the Green's function approach. Finally, some results for a cylindrical electron beam inside a circular waveguide are shown.**

Keywords - Klystron, large-signal analisys, lagrangian approach, disk model, space-charge, Green's function.

I. INTRODUCTION

It is well-known that, in most practical situations involving ensemble of electrons, where it has finite transverse cross section and it may be enclosed in an envelope that could be a drift tube, as found in microwave tubes, like klystrons, traveling-wave amplifiers and gyrotrons, there is a reduction of the plasma-frequency by a factor called plasma-frequency reduction factor [1]. Ratifying its importance, it is used in a one-dimensional numerical code for the study of amplifiers klystrons, based in large-signals conditions and lagrangian approach [2]. There, the plasma-frequency reduction factor is a parameter that is necessary to know before the simulation.

It is possible to avoid the use of this factor if the calculation of the space-charge field already considers that the ensemble of electrons has finite transverse cross section and it is enclosed in an envelope (drift tube, e.g.). One option of space-charge calculation is based on the Green's function approach [3], which is a convenient method of calculating the electrostatic potential in the problems involving distributions of charge as well as boundary values for the potential (i.e., solutions of Poisson's equation).

The assumptions used in the model are:

i) the electron beam is focused by an external static axial magnetic axial which the strength is high enough to guarantee the electron motion be just in axial direction;

ii) the dc velocity of the electron beam is small if compared with light speed. In this conditions the retard potential created by the charge disk motion can be considered as equals to that motionless. Also in this situation the induced magnetic field can be neglected;

iii) the electron beam, considered like a pencil beam, is described by a movement of charge disks, of radius a, without thickness. Each disk is launched in the interaction region, beyond the input plane, considered $z = 0$. Each disk is identified in terms of the relative initial time t_0 to a period of the *RF* modulation signal;

iv) the beam space-charge effects are considered by carried out the electric force over each disk due to the contribution of all the other disks in the interaction region;

v) the dynamics of each individual disk in time t is evaluated considering the space distribution of all other disk in intante time $t - \Delta t$, where Δt is a given integration time step. This approach is know as leap frog; and

vi) the electric charge in each disk is considered uniformly distributed and rigid.

This paper is organized as follows. Section II presents the mathematical formulation of the problem. The numerical results for free space and for an electron beam inside of a circular waveguide are shown in Section III. Finally, the conclusion is presented in Section IV.

II. MATHEMATICAL FORMULATION

The physical interest problem is constituted of an infinite cylindrical electron beam of circular cross section with radius a enclosed in a circular waveguide of radius b. A disk of charge, representative of the set of macro-particles in which the electron beam is divided, is shown in Fig. 1.

It is convenient to assume cylindrical coordinates and propagation in the z direction, due to the geometry.
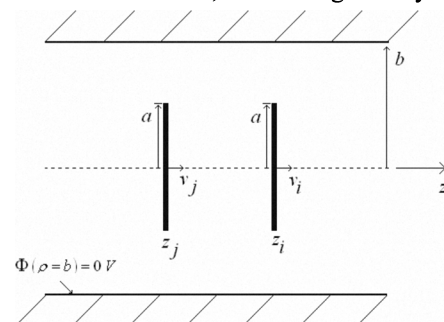

Fig. 1. A disk of charge of radius a inside of a circular waveguide of radius b.

A. The Lagrangian Model

The dynamics of the electron beam can be described from the knowledge of the dynamics of ensemble of disks, and for this purpose, the Newton motion law for each disk must be used.

For this purpose the disk velocity $v_i(t, t_{0i})$ and its axial position $z_i(t, t_{0i})$, for all time instant t, need to be determined. From Newton motion law v_i and z_i are solutions of the first order ordinary differential equation system

$$\begin{cases} \dfrac{dv_i(t, t_{0i})}{dt} = \dfrac{F_{zi}}{m_d} \\ \dfrac{dz_i(t, t_{0i})}{dt} = v_i(t, t_{0i}) \end{cases}, \qquad (1)$$

where m_d is the disk mass and F_{zi} is the total electric force on the i-th disk due to all others disks, in time instant t, in axial positions $z_j(t, t_{0j})$. So F_{zi} can be written as

$$F_{zi} = \sum_{j=1, i \neq j}^{N_d} F_{ij} \left[z_i(t, t_{0i}) - z_j(t, t_{0j}) \right]. \qquad (2)$$

The term in parenthesis denotes the force which is a function of relative positions of each pair of disks. The initial conditions to integration of (1) are:

$$\begin{cases} v_i(t = t_{0i}, t_{0i}) = u_0 \\ z_j(t = t_{0j}, t_{0j}) = 0 \end{cases}, \qquad (3)$$

where u_0 is the initial velocity of the disk. The velocity modulation can be include in the model by using the expression for initial velocity,

$$v_i(t = t_{0i}, t_{0i}) = u_0 \left[1 - \frac{\varepsilon_p}{2} \sin(2\pi f_0 t_{0i}) \right], \qquad (4)$$

where f_0 is the frequency of the RF field modulation in the first microwave cavity, e_p is the modulation index, and the initial time of disk is given by

$$t_{0i} = (i - 1) \frac{T_0}{N_d}, \qquad (5)$$

where $T_0 = 1/f_0$ is the RF field period.

From the solution of (1) under the electric force (2), some relevant field quantities like electron density can be obtained just by taking into account the number of disks located in the position z and $z + \Delta z$ in the time instant t.

B. The Space-Charge Force

In order to carry out the space-charge forces due to charged disks, the Poisson equation for the electrostatic potential $\Phi(\vec{r})$ must be solved,

$$\nabla^2 F(\vec{r}) = -\frac{\rho_v(\vec{r})}{\varepsilon_0}, \qquad (6)$$

subjected to the boundary conditions

$$\begin{cases} F(\rho = b) = 0 \\ F(z = \pm\infty) = 0 \end{cases}. \qquad (7)$$

The charge distribution, $\rho_v(\vec{r})$ is given by

$$\rho_v(\vec{r}) = \begin{cases} \dfrac{q}{\pi a^2} \delta(z - z_j) & \text{if } \rho \leq a \\ 0 & \text{if } a < \rho \leq b \end{cases}, \qquad (8)$$

where q is the electric charge of the j-th infinitely thin disk with radius a at the axial position z_j and ε_0 is free space electric permittivity.

The solution of Poisson equation (6) for boundary conditions (7) and the charge distribution (8) is given, according the Green theorem, by

$$F(\vec{r}) = \frac{1}{\varepsilon_0} \int_V \rho_v(\vec{r}') G(\vec{r}, \vec{r}') d^3\vec{r}', \qquad (9)$$

where $G(\vec{r}, \vec{r}')$ is the Green function for (6) and it satisfies the equation

$$\nabla_r^2 G(\vec{r}, \vec{r}') = -\frac{\delta(\rho - \rho')}{\rho} \delta(\varphi - \varphi') \delta(z - z'), \qquad (10)$$

subjected to homogeneous boundary conditions. In (10) the Dirac delta function $\delta(\vec{r} - \vec{r}')$ is written in a cylindrical coordinate form. A solution of (10) can be found in terms of the ordinary Bessel functions, J_m, of the first kind and m order and its n-th zero, x_{mn}, by noting that

$$f_{mn}(\rho, \varphi) = J_m\left(x_{mn} \frac{\rho}{b}\right) e^{im\varphi}, \qquad (11)$$

is an eigenfunction for the boundary value problem. So in this way the Green function, following the expansion theorem, can be represented as

$$G(\vec{r}, \vec{r}') = \sum_{n=1}^{\infty} \sum_{m=-\infty}^{\infty} g_{mn}(z, \rho', \varphi', z') f_{mn}(\rho, \varphi), \qquad (12)$$

where $g_{mn}(z,\rho',\varphi',z')$, the projection of $G(\vec{r},\vec{r}')$ in a particular eigenfunction, f_{mn}, is given by

$$g_{mn}(z,\rho',\varphi',z') = \int_0^b \int_0^{2\pi} G(\vec{r},\vec{r}')f^*(\rho,\varphi)\rho d\rho d\varphi. \quad (13)$$

The superscript means a complex conjugation. The Green function is written as

$$G(\vec{r},\vec{r}') = \sum_{m=-\infty}^{\infty} \sum_{n=1}^{\infty} \frac{J_m\left(x_{mn}\dfrac{\rho}{b}\right)J_m\left(x_{mn}\dfrac{\rho'}{b}\right)}{2\pi x_{mn}b\left[J_{m+1}(x_{mn})\right]^2}e^{im(\varphi-\varphi')}e^{-\frac{x_{mn}}{b}|z-z'|}. \quad (14)$$

The electric potential can, by integrating (9) using (8) and (14), be expressed as

$$F(\vec{r}) = \frac{q}{a\pi\varepsilon_0}\sum_{n=1}^{\infty}\frac{J_1\left(x_{0n}\dfrac{a}{b}\right)}{\left[x_{0n}J_1(x_{0n})\right]^2}J_0\left(x_{0n}\dfrac{\rho}{b}\right)e^{-\frac{x_{0n}}{b}|z-z_j|}. \quad (15)$$

The electric field can be expressed as the negative gradient of the electric potential (15) as

$$\vec{E}(\vec{r}) = -\nabla F(\vec{r}). \quad (16)$$

Substituting (15) in (16) and carrying through the calculations, observing due to the problem symmetry the only relevant component of the electric field is the axial component, one has

$$E_z(\vec{r}) = \frac{q}{ab\pi\varepsilon_0}\sum_{n=1}^{\infty}\frac{J_1\left(x_{0n}\dfrac{a}{b}\right)}{x_{0n}\left[J_1(x_{0n})\right]^2}J_0\left(x_{0n}\dfrac{\rho}{b}\right)e^{-\frac{x_{0n}}{b}|z-z_j|} \quad (17)$$

Finally, the electrical force acting on the i-th disk charge at z_i due to the j-th disk at z_j can be calculated by

$$F_{ij} = \int_v dq_i(\vec{r})E_z(\vec{r})? \quad (18)$$

where the electric charge $dq_i(\vec{r}) = \rho_i(\vec{r})d^3\vec{r}$, and $\rho_i(\vec{r})$ is given by (8), but now the infinitely thin disk with radius a and charge q is at the axial position z_i. After the calculation one gets, for the force (2), the expression,

$$F_{ij}(|z_i - z_j|) = \frac{2q^2}{\pi a^2\varepsilon_0}\sum_{n=1}^{\infty}\left[\frac{J_1\left(x_{0n}\dfrac{a}{b}\right)}{x_{0n}J_1(x_{0n})}\right]^2 e^{-\frac{x_{0n}}{b}|z_i-z_j|} \quad (19)$$

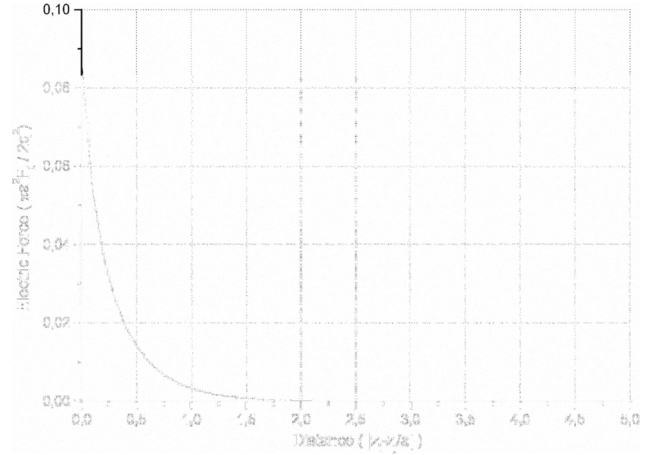Fig. 2 presents the electric force (19) for $b/a = 2$ and as function of the normalized distance $|(z_i - z_j)/a|$.

Fig. 2. Graph of the electric force (19) for $b/a = 2$ and as function of the normalized distance $|(z_i - z_j)/a|$.

Equation (19) constitutes the electric force acting on one disk charge due another disk inside the circular waveguide of radius b. This equation is used to calculate the space-charge forces in this true-$1D$ analysis.

III. NUMERICAL RESULTS

The numerical method must be capable of, for a set of N_D disks, calculate the derivatives of (1) at each step, presenting the new values of each one of the variables. Besides, in the cases where the space-charge field is considered, the force presented in (1) is calculated using (19) at each step, taking into account that the resultant space-charge force on one disk involves the summation of the contributions of all disks (superposition principle).

A. Free Space, with modulation and without space-charge force

In this case, there is a process of modulation in velocity whose responsible for exciting the electron beam is an electric field. At the moment of modulation ($z = 0$), some disks have the velocity increased because they found the electric field in the opposite direction with relation to their directions of propagation and, as consequence, they had been sped up. On the other hand, the disks that found the electric field in the same direction had been decelerated and they have the velocity decreased. Therefore, after the velocity modulation, there are two groups: one is the slow disks and the other is the fast disks. It is emphasized that the velocity of all disks remains constant and equals its modulation value during the entire simulation interval.

Table I presents the quantities [4] used in the numerical code.

TABLE I.   QUANTITIES USED IN THE NUMERICAL CODE

Quantity	Symbol	Value
d.c.beam velocity, m/s	u_0	$4{,}59 \times 10^7$
d.c. beam charge density, C/m^3	ρ_0	$6{,}78 \times 10^{-3}$
d.c. beam current, A	I_0	0,6
frequency, Hz	f_0	$1{,}85 \times 10^9$
disks entrance time interval, s	Δt	$1{,}35 \times 10^{-12}$
permittivity of free space, F/m	ε_0	$8{,}85 \times 10^{-12}$
electron beam radius, mm	a	$7{,}83 \times 10^{-1}$
waveguide radius, mm	b	$15{,}66 \times 10^{-1}$
lenght for density calculation, mm	Δz	$12{,}42 \times 10^{-1}$
number of disks	N_D	1001
modulation index	ε_p	0,1

In the interaction region, as the group of fast disks is modulated by last, these reach the slow group, even without considering the space-charge effect, as it can be seen in the phase space in Fig. 3. As consequence, the density increases until forming one bunch that it is very narrow and has a high current associated with it. Later, the bunch becomes wider and has the highest density associated with the edges [5].
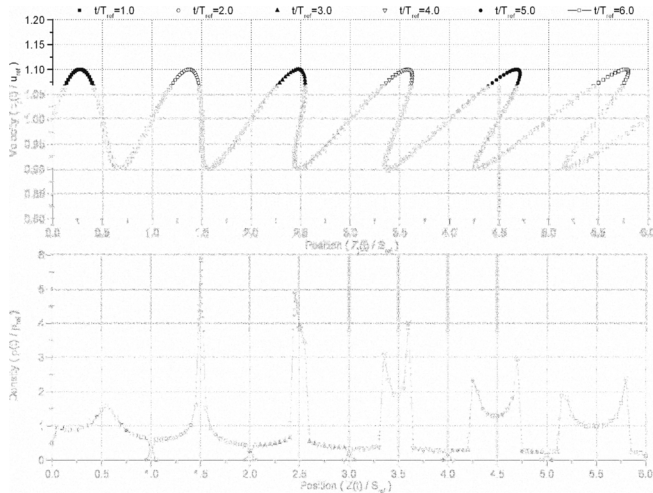

Fig. 3. Phase space of some disks and density in the interaction region for the normalized times: 1.0, 2.0, 3.0, 4.0, 5.0 and 6.0.

Beyond of electron bunch, as the consequence of disks approach one to others, Fig.4 shows the occurrence of the electron overtaking.

B. Free Space, with modulation and space-charge force

In this case, the disks try, in $z = 0$, the modulation in velocity and, after that, in the interaction region, they move under the action of the space-charge force as the resultant force. It should be noted that the disks have their velocities changing
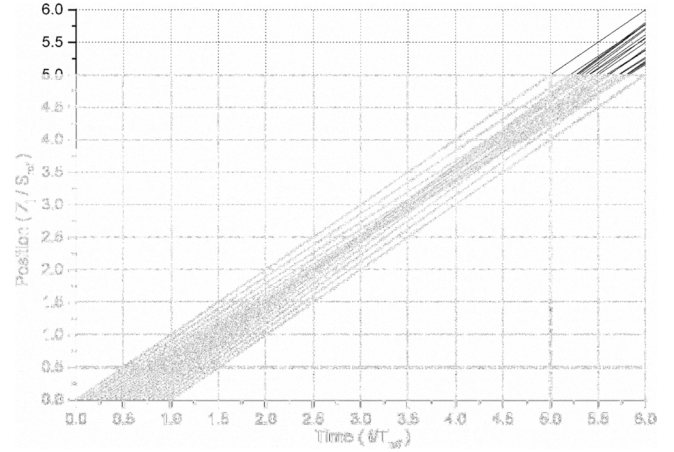

Fig. 4. Trajectories of some disks in the interaction region.

in the interaction region, as it can be seen in the phase space in Fig. 5.

Again, as consequence of two groups of disks (slow and fast), the density increases until forming one bunch that it is very narrow as it can be seen in the Fig. 5 but, in this case, the highest density occurs later and it is higher than the previous case. Later, the bunch becomes wider and has the highest density associated with the edges.
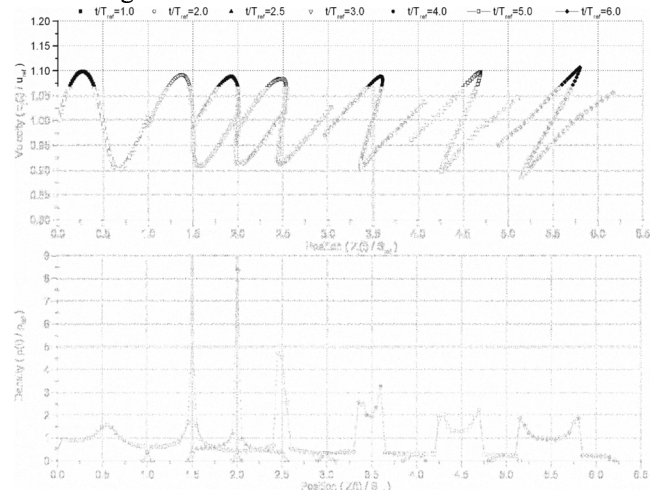

Fig. 5. Phase space of some disks and density in the interaction region for the normalized times: 1.0, 2.0, 2.5, 3.0, 4.0, 5.0 and 6.0.

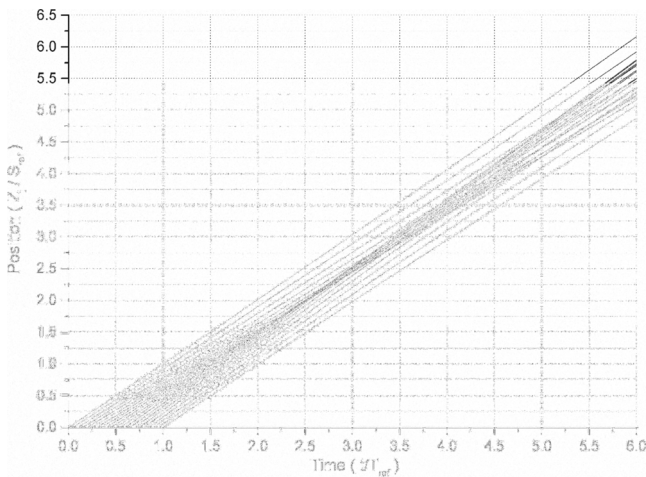Fig. 6 shows the electron bunch and the electron overtaking.

Fig. 6. Trajectories of some disks in the interaction region.

C. Waveguide, without modulation and with space-charge force

In this case, the disks move, in the interaction region, under the action of the space-charge force, which is the resultant force. It is verified clearly in Fig. 7 that throughout the time some disks that have entered first in the interaction region are sped up because its resultant space-charge force has the same direction related to their directions of propagation. On the other hand, some disks are decelerated because its resultant space-charge force has the oposite direction related to its direction of propagation. As consequence, the density decreases, as it can be seen in the Fig. 7. It should be noted that initially the decrease is more intense with extreme disks. At the same time, the distances between these disks increase from the entrance ($z = 0$), as it can be seen in the Fig. 8.
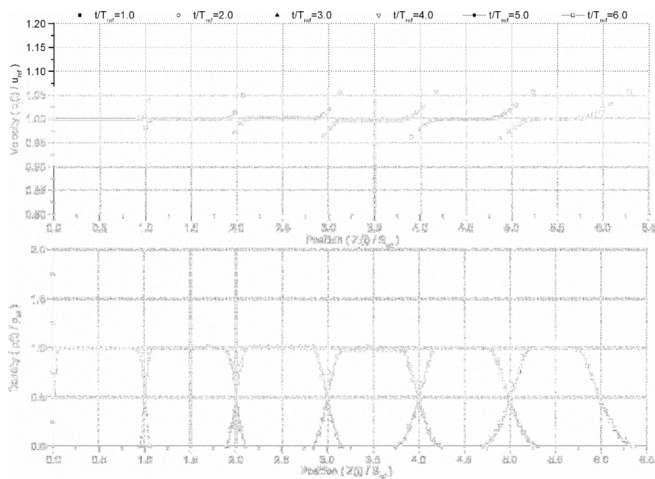
Fig 7 shows that, at the moment which the distances between all disks become relevant, there is a significant decrease of the density. Besides, it is possible to infer from the graph of Fig. 8 that there is not electron bunching.
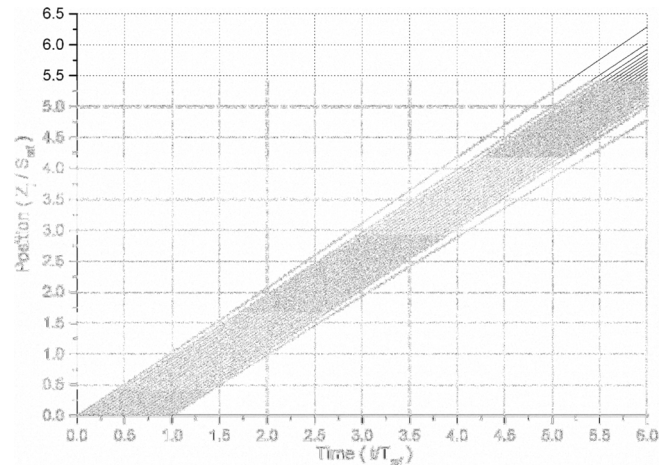

Fig. 8. Trajectories of some disks in the interaction region.

D. Waveguide, with modulation and space-charge force

In this case, the disks try, in $z = 0$, the modulation in velocity and, after that, in the interaction region, they move under the action of the space-charge force, which is the resultant force. It is important to observe that the disks have its velocities changing in the interaction region, as it can be seen in the phase space in fig. 9. Again, as consequence of two groups of disks (slow and fast), the density increases until forming one bunch that it is very narrow and, therefore, has a high current associated with it, as it can be seen in the Fig. 9 but, in this case, the highest density occurs earlier and it is lower than the item B (free space). Later, the bunch becomes wider and decreases in different way them previous cases.

Fig. 7. Phase space of some disks and density in the interaction region for the normalized times: 1.0, 2.0, 3.0, 4.0, 5.0 and 6.0.
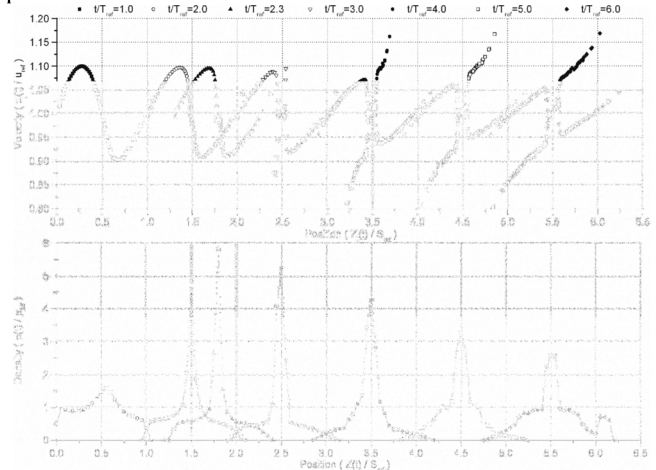

Fig. 9. Phase space of some disks and density in the interaction region for the normalized times: 1.0, 2.0, 2.3, 3.0, 4.0, 5.0 and 6.0.

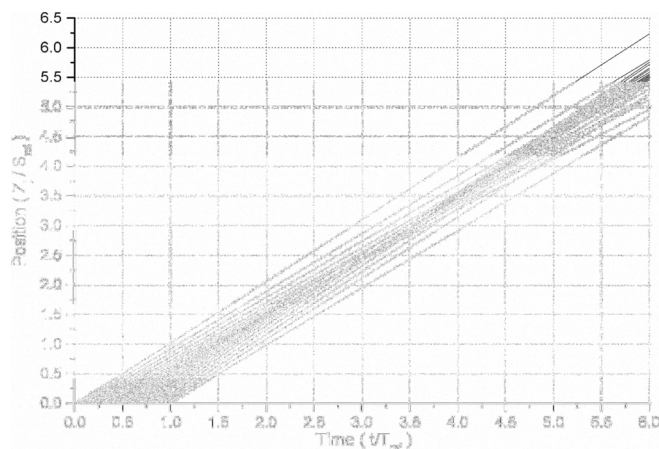Fig. 10 shows that the electron bunch phenomenon occurs in this case as well as the electron overtaking.

Fig. 10. Trajectories of some disks in the interaction region.

IV. CONCLUSION

In this work a real 1D analysis of a klystron amplifier was presented. It was considered real because, instead of using the plasma-frequency reduction factor, was present the calculation of the space-charge force using the Green's function approach. The results described in reasonable way the dynamics of the electron beam in the interaction region, validating the mathematical formulation and code developed.

REFERENCES

[1] R. K. Silva, C.C.Motta, "An alternative approach for the calculation of the plasma-frequency reduction factor," *MOMAG2008* , v. 1., pp. 654-658, Sep 2008.

[2] R. K. Silva, C.C.Motta, "A Large-signal analysis of klystron amplifier," *MOMAG2008* , v. 1., pp. 990-994, Sep 2008.

[3] J. D. Jackson, Classical Electrodynamis, 2nd ed.. New York: John Wiley & Sons, 1975.

[4] J. G. Wöhlbier, J. H. Booske, "Nonlinear space-charge wave theory of distortion in a klystron," *IEEE Trans. Electron Devices*, vol. 52, no.5, pp. 734-741, May 2005.

[5] K.R. Spangenberg, Vacuum Tubes International Student Edition. Tokyo: Kogakuska, 1948, ch. 17.